Young's Modulus for Laminated Machine Structures With Particular Reference to Switched Reluctance Motor Vibrations

Zhangjun Tang, *Member, IEEE*, Pragasen Pillay, *Senior Member, IEEE*, Avoki M. Omekanda, *Senior Member, IEEE*, Chen Li, and Cetin Cetinkaya

***Abstract*—The switched reluctance motor (SRM) has a disadvantage of higher acoustic noise, caused by stator vibrations. Techniques for noise reduction require knowledge of the modal frequencies, which depend on mechanical shapes and dimensions as well as material properties, for example, Young's modulus, Poisson's ratio, mass density, etc. It is found that the generally accepted value of Young's modulus is not valid for a machine with laminations and no frame. This paper introduces a simple and nondestructive method for the measurement of Young's modulus; it is then used in a finite-element (FE) program to determine the resonant frequencies of SRM stator vibration. The effects of mass density and Poisson's ratios are also discussed. The FE results are validated by vibration tests, which show good accuracy.**

***Index Terms*—Switched reluctance motor (SRM), vibration, Young's modulus.**

I. Introduction

VIBRATION and acoustic noise in the switched reluctance motor (SRM) is caused by the ovalizing deformation of the stator lamination stack due to its radial magnetic attraction to the rotor [1]. This is a big disadvantage for industrial applications. There are several ways of determining stator resonant frequencies and mode shapes of the SRM: analytical calculations, numerical computation (usually by the finite-element (FE) method), and/or experimental measurements [2]. There is considerable advantage and interest in using numerical methods for the computation of resonant frequencies and mode shapes during motor design. The material properties, like mass density and Young's modulus, are key factors besides stator dimensions and shapes. In the approximate formula for stator natural frequency, the stator resonant frequency has the relation [3]

$$f_r \propto \sqrt{\frac{E}{\rho}} \tag{1}$$

where f_r is the stator natural frequency, and E and ρ are the Young's modulus and mass density of the stator material, respectively.

The density of the lamination core can be easily determined, however, Young's modulus deserves some consideration. The Young's modulus value of stainless steel ($E = 2.07 \times 10^{11}$ N/m^2) has been widely used by researchers in electric machine vibrations area. However, in order to allow theoretical prediction to converge to experimental results, some researchers even varied the value until the predicted natural frequencies converged to the measured values. The fact is that the stator lamination steel of an electric machine is different from stainless steel; in addition, the material properties may change during core lamination or motor manufacturing. Because of the important role it plays in the determination of stator natural frequencies and its complexity, the treatment of Young's modulus has to be considered seriously.

This paper introduces a nondestructive method of Young's modulus measurement. FE analysis is then used to determine resonant frequencies of two different motor configurations. The results are validated by vibration tests.

II. Young's Modulus Measurement

A. Methodology

Many useful mechanical properties of materials, like Young's modulus, are obtained from tension tests and/or compression tests [5]. However, these tests are not trivial for an electric machine stator. Firstly, the force load may change the electromagnetic properties of the stator laminations. Secondly, the test may damage the stator lamination and/or windings. Finally, the odd shape of an electric machine stator makes it difficult for mounting.

The other method widely used by mechanical and material researchers is an ultrasonic method, which is nondestructive. This is especially good for an electric machine. It will be discussed in detail in this paper.

Paper IPCSD 04–011, presented at the 2003 IEEE International Electric Machines and Drives Conference, Madison, WI, June 1–4, and approved for publication in the IEEE TRANSACTIONS ON INDUSTRY APPLICATIONS by the Electric Machines Committee of the IEEE Industry Applications Society. Manuscript submitted for review March 28, 2003 and released for publication February 9, 2004. This work was supported by Delphi Research Labs, Shelby Township, MI.

Z. Tang is with Stryker Instruments, Kalamazoo, MI 49001 USA (e-mail: ztang@inst.strykercorp.com).

P. Pillay is with the Department of Electrical and Computer Engineering, Clarkson University, Potsdam, NY 13699 USA (e-mail: pillayp@clarkson.edu).

A. M. Omekanda is with Delphi Research Labs, Shelby Township, MI 48306 USA (e-mail: avoki.omekanda@delphi.com).

C. Li and C. Cetinkaya are with the Mechanical Engineering Department, Clarkson University, Potsdam, NY 13699 USA.

Digital Object Identifier 10.1109/TIA.2004.827460

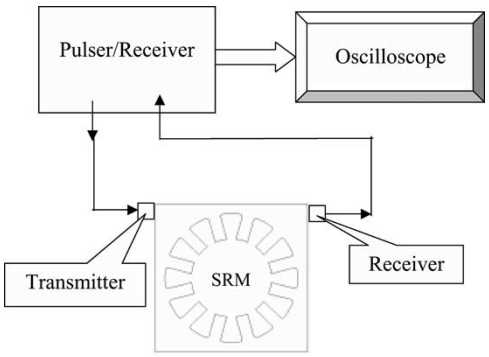

Fig. 1. Block diagram of ultrasonic method.

The ultrasonic technique is a method for measuring the elastic properties of a material. The sample to be measured is placed between an ultrasonic transmitter (pulser) and receiver, and the time for an ultrasonic pulse to traverse the media between the transducers is measured. The block diagram is shown in Fig. 1.

Stress waves from 20 Hz to 20 kHz are perceived as sound. Waves above 20 kHZ are referred to as ultrasonic; ultrasonic frequencies between 1–10 MHz are commonly used in the nondestructive evaluation of engineering materials, for materials characterization.

Ultrasonic wave speed, c, depends on the stiffness and on the density, ρ, of the materials under study [6], [7]. For longitudinal waves

$$c = \sqrt{\frac{E}{\rho}} \tag{2}$$

where E is the Young's modulus. This is valid for a long homogeneous rod of length much longer than the wavelength, and width much less than the wavelength. If the width is much larger than the wavelength, then wave speed is governed by the tensorial modulus

$$c = \sqrt{\frac{1-\upsilon}{(1+\upsilon)(1-2\upsilon)}\frac{E}{\rho}} \tag{3}$$

where υ is the Poisson's ratio. The test motor stator used in this paper belongs to this category. Therefore, the Young's modulus of the motor stator can be described as

$$E = \frac{(1+\upsilon)(1-2\upsilon)}{(1-\upsilon)}\rho c^2. \tag{4}$$

Velocity (wave speed c) can be measured by determining the time delay for the wave to pass through a sample of material. The velocity is the distance (thickness) divided by the time delay. In this method, one transducer sends the waves and another one receives them.

B. Test Setup

The prototype SRM used in this paper is shown in Fig. 2 (the stator part with windings). Fig. 3 shows the above-described ultrasonic method that is used to measure Young's modulus of this 12/8 three-phase SRM stator core lamination. A 200-MHz computer-controlled pulser/receiver together with two transducers (KB-Aerotech, GAMA 2.25 MHz/.50) are used. The test data

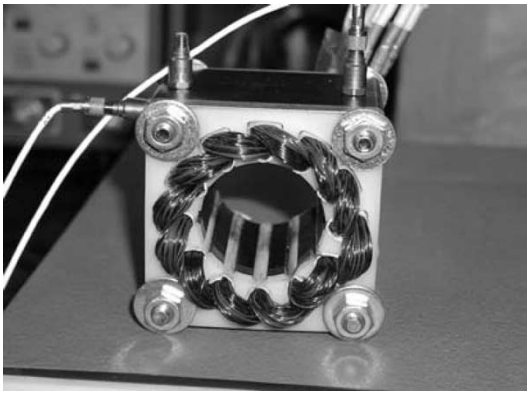

Fig. 2. Stator of the prototype SRM.

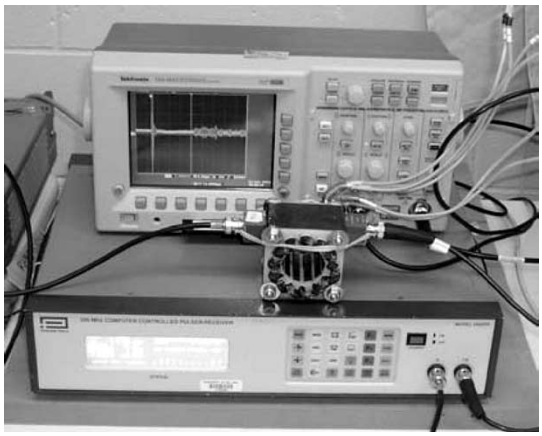

Fig. 3. Test setup.

are then recorded in a digital oscilloscope and analyzed in a computer program to obtain the wave speed and Young's modulus. The placement of the transmitter and receiver is important, as shown in Fig. 3. An air gap between the transmitter and receiver should be avoided.

Compared with the traditional tension /compression method, the ultrasonic method has several advantages. Firstly, it is fast, convenient, and simple and no special hydraulic equipment is needed. Secondly, no special mounting is needed: the transducers are attached to the test object where needed. Then, no damage is done to the stator or to the windings. Finally, it is easy to change the test location, for example, in the horizontal direction or vertical direction, or from the inner side of the stator pole.

C. Test Results

Fig. 4 records the travel time of the ultrasonic signal inside the stator core lamination. The wave speed c can then be calculated, knowing the length of the test object (SRM stator). Using (4), Young's modulus E of the stator lamination is obtained in both the vertical and horizontal directions (as viewed in Fig. 2), where Poisson's ratio $\upsilon = 0.3$ [4]–[6], mass density $\rho = 0.935 \times 7.8 \times 10^3$ kg/m^3, and 0.935 is the stacking factor (generally, it is $0.92 \sim 0.95$) of the stator core lamination. The measured value is 1.521×10^{11} N/m^2, and is the same in both directions, quite different from 2.07×10^{11} N/m^2 used by most researchers. The laminated structure is not as stiff as a solid

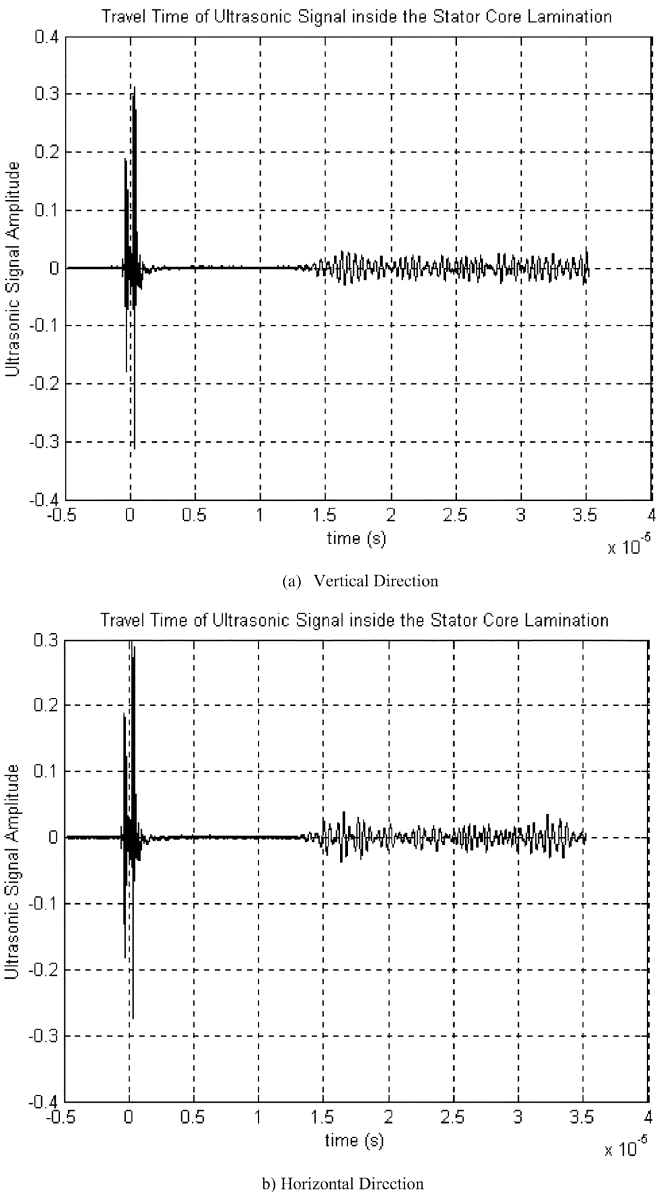

Fig. 4. Travel time of ultrasonic signal inside the stator core lamination.

TABLE I
MEASURED YOUNG'S MODULUS

Poisson's Ratio υ	Young's Modulus E ($\times 10^{11}$N/m^2)
0.3 (Commonly Used)	1.521
0.27	1.638
0.34	1.371
0 (One-dimensional)	2.047

steel structure, hence, the lower measured value. The measurement from corner to corner was not done because the ultrasonic wave would travel through the air and, hence, produce incorrect results.

Several different Poisson's ratio values are used to calculate Young's modulus, which are listed in Table I. They are used later in an FE program for determination of resonant frequencies for comparison purposes.

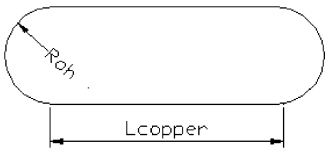

Fig. 5. One turn of the coil.

III. CALCULATION RESULTS

A. Equivalent Mass Density Determination

The effect of phase windings on the vibration of electric machines has been discussed by many studies [9]–[11]. Generally, it is believed that the windings have effects of both additional mass and vibration damping on the vibrational behavior of electric machines. In this paper, the mass of phase windings is treated as an increase of the mass density of the pole to which the winding is attached. According to [11], the concentrated windings of the SRM are installed on the stator poles. There is insulation between a pole and winding. For conventional motors, the contact between pole and winding assembly is tight enough to allow the windings to move with the pole, but cannot add an extra stiffness due to the existence of the insulation. Although the windings may contribute to stiffness if the slot fill factor is high, the increase in the stiffness is low when compared to the mass added by the windings to the stator assembly. Therefore, the effect of windings is equated to an increase of the pole mass. As a result, the geometrical model for FE computation is the same as the model without considering the winding effect, but the poles are treated as a different material with specific mass density. The equivalent mass density of the pole with winding effect will be explained explicitly as follows.

The equivalent mass density ρe can be expressed as $\rho_e = (m_{\rm pole} + m_{\rm coil})/V_{\rm pole}$, where $m_{\rm pole}$ is the mass of one pole, $m_{\rm coil}$ is the mass of the coil attached to one pole, $V_{\rm pole}$ is the volume of the pole.

The volume of the pole $V_{\rm pole} = L_{\rm stack} \times H_{\rm pole} \times W_{\rm pole}$, where $L_{\rm stack}$ is the length of the pole (which is the same as stator stack length), $H_{\rm pole}$ is the height if the pole and $W_{\rm pole}$ is the width of the pole.

The mass of one pole is $m_{\rm pole} = \rho_{Fe} \times f_{\rm stack} \times V_{\rm pole}$, where ρ_{Fe} is the mass density of steel, and $f_{\rm stack}$ is the stacking factor of the stator lamination, which is generally $0.92 \sim 0.95$.

The mass of the coil can be calculated as $m_{\rm coil} = N_{\rm turn} \times m_{\rm turn}$, where $N_{\rm turn}$ is the turns of winding per pole and $m_{\rm turn}$ is the mass of each turn. The mass of each turn of the coil $m_{\rm turn} = \rho_{\rm cu} \times L_{\rm turn} \times A_{\rm turn}$, where $\rho_{\rm cu}$ is the mass density of copper, $L_{\rm turn}$ is the length of each turn and $A_{\rm turn}$ is the intersection area of copper wire. Fig. 5 shows the shape of one turn of the coil, from which the length of each turn can be calculated, $L_{\rm turn} = 2\pi R_{oh} + 2L_{\rm copper}$, where R_{oh} is the radius of the winding overhang, $L_{\rm copper}$ is the length of the straight line shown in Fig. 5, which is longer than the stator stack length. The intersection area of copper wire can be calculated as $A_{\rm turn} = \pi(D_{\rm barewire}/2)^2$, where $D_{\rm barewire}$ is the diameter of the bare copper wire with corresponding A.W.G.

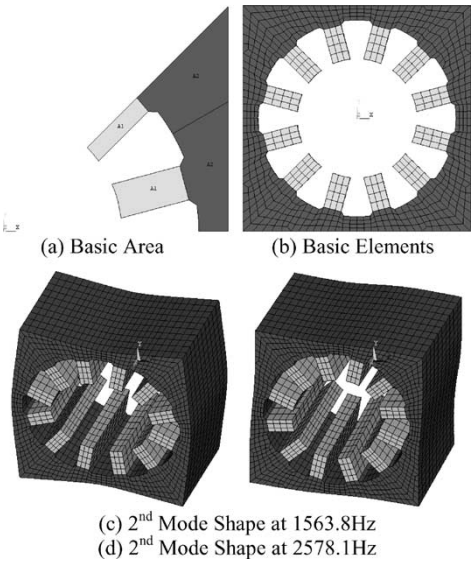

Fig. 6. FE basic area, mesh, and second-order mode shapes (with measured Young's modulus).

Finally, the equation for equivalent mass density of the pole is (5), as shown at the bottom of the page.

The equivalent density of the pole is 20.29×10^3 kg/m^3.

B. FE Analysis

A three–dimensional (3-D) FE model is constructed for this motor, as shown in Fig. 6(a) and (b), which shows the basic areas and elements used in the FE model. The measured Young's modulus E is used with the ANSYS 3-D model to determine the natural frequencies, with the second modes being at 1563.8 Hz (side-to-side mode shape) and 2578.1 Hz (corner-to-corner mode shape).

The commonly used Young's modulus (2.07×10^{11} N/m^2) is also used in the FE program to re-evaluate the resonant frequencies. Both are given in Table II. To evaluate the effect of Poisson's ratio on the resonant frequencies, a different Poisson's ratio value, $\upsilon = 0.34$ and 0.27 [6], [12], is used in the FE program, with all the other material properties kept the same. No effect has been observed by changing this value.

IV. Experimental Validation

In order to validate the FE calculations of resonant frequencies, a force hammer test is carried out for the SRM. Fig. 7 shows the time-domain hammer impulse force, damped transient stator acceleration, and frequency-domain acceleration. It can be seen clearly that the second mode resonant frequencies ([3], [11] and [13]), which are 1497 and 2655 Hz, respectively, are very close to the calculated ones with the measured Young's modulus (the peak of 2095 Hz appearing in this figure is the resonant frequency of the test setup). The errors between the calculated and measured resonant frequencies are less than 4.5% for both resonant frequencies, as shown in Table II, row 1). The errors of the calculated resonant frequencies using commonly used Young's modulus are 21.9% and 13.3%, respectively, as listed in Table II, row 2).

V. Comparisons

The effects of Young's modulus, equivalent mass, Poisson's ratio, and stator core lamination stacking factor on the resonant frequencies are studied. These results are compared with impulse hammer test results, as shown in Table II.

Row 1) shows the calculated resonant frequencies with measured Young's modulus, commonly used Poisson's ratio, consideration of winding effect, and stacking factor. Both errors are less than 4.5% compared with the impulse force hammer tests.

Row 2) shows the calculated results with commonly used Young's modulus (2.07×10^{11} N/m^2), the calculation errors (21.9% and 13.3%, respectively) are not acceptable although the winding effect and stacking factor are considered.

Rows 3), 4), and 5) show the effect of Poisson's ratio on the resonant frequencies; no major effect has been found. The Poisson's ratio $\nu = 0$ here refers to the so-called "one-dimensional" material.

Rows 6), 7), and 8) show the role of Poisson's ratio on the accurate determination of Young's modulus during ultrasonic measurements, which is based on (4). Comparing with row 1), the commonly used Poisson's ratio $\nu = 0.3$ has the best result, while $\nu = 0.27$ and 0.34 have acceptable results; both errors are around 8%. $\nu = 0$, which refers to homogeneous one-dimensional structure, leads to 20% error. The Young's modulus determination of electric machine stators cannot be treated as a homogeneous structure.

Row 9) reveals the effect of stator core lamination stacking factor on the resonant frequency. The properties of stacked lamination are definitely different from that of iron or steel, as can be seen from the Young's modulus measurements. The existence of stacking factor will change the mass of the object, hence, the resonant frequencies.

Rows 10) and 11) are the calculated results with commonly used Young's modulus without considering winding effects [13]. This is a commonly used method during the electric machine design stage because of the lack of winding parameters. The results reveal the fact that winding effects cannot be neglected, otherwise, unacceptable errors will occur. In row 10), errors of 56.6% and 36.4% occur when neglecting the stacking factor, and in row11), errors are 62.0% and 41.1% when considering the stacking factor. The calculation results are still unacceptable if winding effects are not considered, even though a correct Young's Modulus is used, as seen in row 12), where errors are 38.9% and 20.9% for the two second mode frequencies.

$$\rho_e = \frac{\rho_{Fe} \cdot f_{\text{stack}} \cdot (L_{\text{stack}} \cdot H_{\text{pole}} \cdot W_{\text{pole}}) + N_{\text{turn}} \cdot \left\{ \rho_{\text{cu}} \cdot (2\pi R_{oh} + 2L_{\text{stack}}) \cdot \left[\pi \left(\frac{D_{barewire}}{2} \right)^2 \right] \right\}}{(L_{\text{stack}} \cdot H_{\text{pole}} \cdot W_{\text{pole}})} \tag{5}$$

TABLE II
EFFECT OF YOUNG'S MODULUS ON THE RESONANT FREQUENCIES OF THE SECOND MODE SHAPES

	E	ρ_1	ρ_2	υ	f_2	f_2 (error %)	f_2'	f_2' (error %)
1)	**1.521**	**20.29**	**7.8×0.935**	**0.3**	**1563.8**	**4.5**	**2578.1**	**-2.9**
2)	2.07	20.29	7.8×0.935	0.3	1824.3	21.9	3007.7	13.3
3)	1.521	20.29	7.8×0.935	0.27	1562.9	4.4	2577.4	-2.9
4)	1.521	20.29	7.8×0.935	0.34	1565.1	4.6	2579.2	-2.9
5)	1.521	20.29	7.8×0.935	0	1558.6	4.1	2573.2	-3.1
6)	1.638	20.29	7.8×0.935	0.27	1621.9	8.3	2674.7	0.7
7)	1.371	20.29	7.8×0.935	0.34	1485.9	-0.7	2448.7	-7.8
8)	2.047	20.29	7.8×0.935	0	1808.1	20.8	2985.7	12.5
9)	1.627	20.80	7.8	0.3	1586.4	6.0	2608.6	-1.7
10)	2.07	7.8	7.8	0.3	2344.9	56.6	3621.3	36.4
11)	2.07	7.8×0.935	7.8×0.935	0.3	2425.1	62.0	3745.0	41.1
12)	1.521	7.8×0.935	7.8×0.935	0.3	2078.8	38.9	3210.2	20.9
13)	1.521	28.59	7.8×0.935	0.3	1383.5	-7.6	2326.7	-12.4

Note: The measured second resonant frequencies are 1497 and 2655 Hz, respectively (see also Section VI), which are used as the basis for calculating the percentage errors.

E = Young's modulus ($\times 10^{11}$ N/m^2)

ρ_1 = mass density of stator pole ($\times 10^3$ kgm^3)

ρ_2 = mass density of stator core lamination ($\times 10^3$ kg/m^3)

ν = Poisson's ratio

f_2, f_2' = second mode resonant frequencies

0.935 is the stator core lamination stacking factor (generally, it is $0.92 \sim 0.95$)

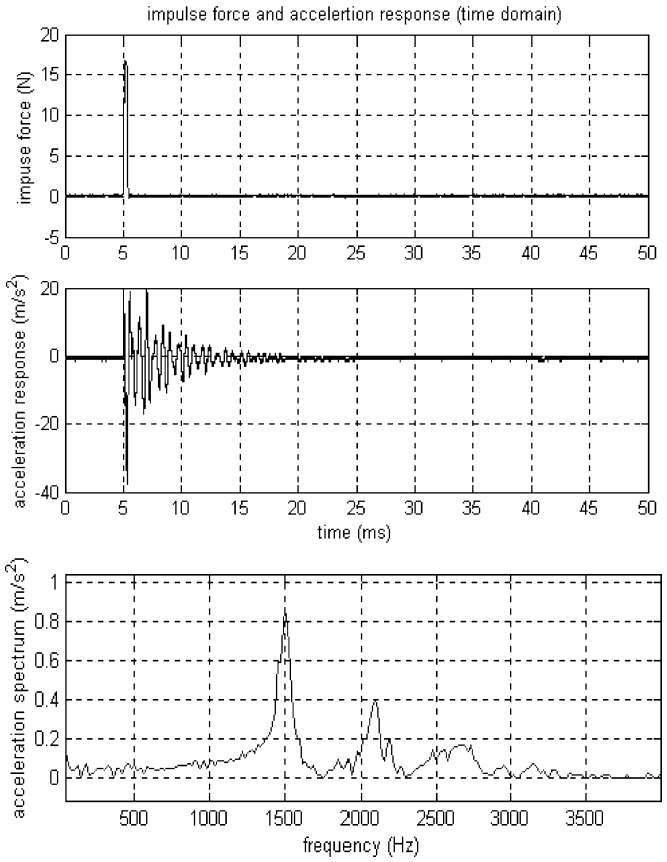

Fig. 7. Force hammer test result: force impulse and stator acceleration.

Row 13) describes an easily made mistake when determining the equivalent mass density of the stator pole—using the total wire diameter instead of the bare wire diameter (notice that there is an insulation layer for winding copper wires), hence increasing the equivalent mass and lowering the resonant frequencies.

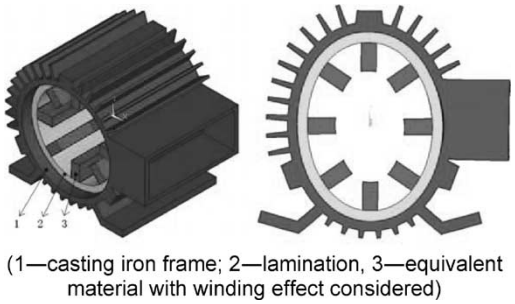

Fig. 8. 3-D FE model and second mode shape.

VI. STUDY ON A SECOND SRM

A 4-kW 8/6 SRM is used as a second motor in this paper to study the effects of material properties. Fig. 8 shows the 3-D FE model and a second mode shape (end-bells and rotor are not included). Different materials properties are used in the FE model to calculate the second mode resonant frequency, which are then compared to the measured value. The measured second mode resonant frequency is 1060.4 Hz. This is used as a basis for calculating errors. Table III shows the FE calculation results with different material properties.

As shown in Table III, Case 3 (measured Young's Modulus 1.521×10^{11} N/m^2 used, with winding effect, with stacking factor considered) does not change the resonant frequency as much as that in the 12/8 SRM described above. This means that the Young's modulus is less important for the determination of resonant frequencies in the SRM with a cast iron frame. Case 4 shows again that winding effects have to be considered.

TABLE III
EFFECT OF MATERIAL PROPERTIES ON OULTON SRM

	Case 1	Case 2	Case 3	Case 4
f_2 (Hz)	1040.6	1054.9	1027.9	1369.7
f_2 (Error %)	-1.9	-0.5	-3.1	29.2
E_1 ($\times 10^{11}$ N/m^2)	1.6	1.6	1.6	1.6
ν_1	0.275	0.275	0.275	0.275
ρ_1 ($\times 10^3$ kg/m^3)	7.8	7.8	7.8	7.8
E_2 ($\times 10^{11}$ N/m^2)	2.07	2.07	1.521	2.07
ν_2	0.3	0.3	0.3	0.3
ρ_2 ($\times 10^3$ kg/m^3)	18.59	18.083	18.083	7.293
E_3 ($\times 10^{11}$ N/m^2)	2.07	2.07	1.521	2.07
ν_3	0.3	0.3	0.3	0.3
ρ_3 ($\times 10^3$ kg/m^3)	7.8	7.293	7.293	7.293

Note:

Case 1—Commonly used material properties, with winding effects;

Case 2—Commonly used material properties, with winding effects and with stacking factor considered;

Case 3—Measured Young's Modulus used, with winding effects and with stacking factor considered;

Case 4—Commonly used material properties, without winding effects and with stacking factor considered.

VII. CONCLUSION

A convenient and nondestructive method for the measurement of Young's modulus of stacked laminations in electric motor stators was introduced in this paper. It shows the importance of Young's modulus in the calculation of stator resonant frequencies. The commonly used Young's modulus value is not appropriate for the calculation of resonant frequencies in the motor without a frame, however, lower errors are produced for the motor with frame. The results were validated by a 3-D FE calculation together with force hammer vibration tests.

The Poisson's ratio is important for determining the Young's modulus using ultrasonic tests. It is necessary to include the stator core lamination stacking factor, the winding effects, together with the appropriate Young's modulus value for resonant frequencies determination during the design phase of SRMs.

It seems that the Young's modulus of the lamination stack is less important for the determination of resonant frequencies in the SRM with a cast iron frame. However, more rigorous investigations need to be done, for motors of different sizes, different configurations, different types, etc.

REFERENCES

[1] D. E. Cameron, J. H. Lang, and S. D. Umans, "The origin and reduction of acoustic noise in doubly salient variable-reluctance motors," *IEEE Trans. Ind. Applicat.*, vol. 28, pp. 1250–1255, Nov./Dec. 1992.

[2] P. Vijayraghavan and R. Krishnan, "Noise in electric machines: A review," *IEEE Trans. Ind. Applicat.*, vol. 35, pp. 1007–1013, Sept./Oct. 1999.

[3] R. S. Colby, F. Mottier, and T. J. E. Miller, "Vibration modes and acoustic noise in a 4-phase switched reluctance motor," *IEEE Trans. Ind. Applicat.*, vol. 32, pp. 1357–1364, Nov./Dec. 1996.

[4] S. A. Long, Z. Q. Zhu, and D. Howe, "Vibration behavior of stators of switched reluctance motors," *Proc. IEE—Elect. Power Applicat.*, vol. 148, no. 3, pp. 257–264, May 2001.

[5] R. R. Craig JR., *Mechanics of Materials*. New York: Wiley, 1996.

[6] W. M. Lai, D. Rubin, and E. Krempl, *Introduction to Continuum Mechanics*. Burlington, MA: Butterworth-Heinemann, 1993.

[7] K. F. Graff, *Wave Motion in Elastic Solids*. New York: Dover, 1975.

[8] C. Cetinkaya, "Localization of longitudinal waves in Bi-periodic elastic structures with disorder," *J. Sound Vib.*, vol. 221, no. 1, pp. 49–66, 1999.

[9] S. P. Verma and R. S. Girgis, "Method for accurate determination resonant frequencies and vibration behavior of stators of electrical machines," *Proc. Inst. Elect. Eng.*, pt. B, vol. 128, no. 1, pp. 1–11, Jan. 1981.

[10] C. Yongxiao, W. Jiahua, and H. Jun, "Analytical calculation of natural frequencies of stator of switched reluctance motor," in *Proc. IEE EMD'97*, Sept. 1–3, 1997, pp. 81–85.

[11] W. Cai, P. Pillay, and Z. Tang, "Impact of stator windings and end bells on resonant frequencies and mode shapes of switched reluctance motors," *IEEE Trans. Ind. Applicat.*, vol. 38, pp. 1027–1036, July/Aug. 2002.

[12] Z. Q. Zhu, L. Xu, and D. Howe, "Influence of mounting and coupling on the natural frequencies and acoustic noise radiated by a PWM controlled induction machine," in *Proc. 9th Int. Conf. Electrical Machines and Drives (EMD99)*, Canterbury, U.K., Sept. 1–3, 1999, pp. 164–168.

[13] W. Cai, P. Pillay, and A. Omekanda, "Low vibration design of SRM's for automotive applications using modal analysis," in *Proc. IEEE IEMDC*, Boston, MA, June 2001, pp. 261–266.

[14] J. Mahn, D. Williams, P. Wung, G. Horst, J. Llooyd, and S. Randall, "A systematic approach toward studying noise and vibration in switched reluctance machines: Preliminary results," in *Conf. Rec. IEEE-IAS Annu. Meeting*, San Diego, CA, Oct. 6–10, 1996, pp. 779–785.

Zhangjun Tang (S'00–M'03) received the B.S. degree in electrical engineering from Harbin Institute of Technology, Harbin, China, in 1994, the M.S. degree from Beijing Institute of Control Devices, Beijing, China, in 1997, and the Ph.D. degree from Clarkson University, Potsdam, NY, 2002.

Following receipt of the M.S. degree, he spent 2 1/2 additional years at Beijing Institute of Control Devices, developing gyroscope motor and control systems for various navigation platforms. In September 2002, he joined Stryker Instruments, Kalamazoo, MI, as a Senior Design Engineer in the Powertools Product Platform Research and Development Group. His research interests include design, control, and modeling of electrical machines and drives, numerical computation of electromagnetic fields and mechanical structures, and vibration and noise of electrical machines.

Pragasen Pillay (S'84–M'87–SM'92) received the Bachelor's degree from the University of Durban-Westville, Durban, South Africa, in 1981, the Master's degree from the University of Natal, Durban, South Africa, in 1983, and the Ph.D. degree from Virginia Polytechnic Institute and State University, Blacksburg, in 1987.

From January 1988 to August 1990, he was with the University of Newcastle-upon-Tyne, U.K. From August 1990 to August 1995, he was with the University of New Orleans. Currently, he is with Clarkson University, Potsdam, NY, where he is a Professor in the Department of Electrical and Computer Engineering and holds the Jean Newell Distinguished Professorship in Engineering. He is also an Adjunct Professor at the University of Cape Town, Cape Town, South Africa. His research and teaching interests are in modeling, design, and control of electric motors and drives for industrial and alternate energy applications.

Dr. Pillay is a member of the IEEE Power Engineering, IEEE Industry Applications (IAS), IEEE Industrial Electronics, and IEEE Power Electronics Societies. He is a member of the Electric Machines Committee and Past Chairman of the Industrial Drives Committee of the IAS and Past Chairman of the Induction Machinery Subcommittee of the IEEE Power Engineering Society. He currently chairs the Awards Committee of the IAS Industrial Power Conversion Department. He has organized and taught short courses in electric drives at IAS Annual Meetings. He is a Fellow of the Institution of Electrical Engineers, U.K., and a Chartered Electrical Engineer in the U.K. He was also a recipient of a Fulbright Scholarship.

Avoki M. Omekanda (M'95–SM'97) received the bachelor's degree in physics from Mohammed V University, Rabat, Morocco, in 1984, and the Engineer and Ph.D. degrees in electrical engineering from the Faculté Polytechnique de Mons, Mons, Belgium, in 1987 and 1993, respectively.

Following the receipt of the Engineer's diploma, he worked for A.C.E.C Corporation, Charleroi, Belgium. In January 1990, he joined the Faculté Polytechnique de Mons as a Research Engineer. His research interests included computer-aided design for switched reluctance machines and magnetic field computation using numerical methods. After receiving the Ph.D. degree, he was an Assistant Professor in the Electrical Engineering Department, Faculté Polytechnique de Mons, for two years. In June 1995, he joined the General Motors Research and Development Center, Warren, MI, as a Senior Research Engineer. In 1999, he became part of Delphi Research Labs, Shelby Township, MI, where he is currently a Staff Research Engineer. His research interests include design, analysis, and control of electric machines, in particular, switched reluctance, for automotive applications.

Dr. Omekanda is a Member of the Association des Ingénieurs de Mons (Belgium) and Société des Electriciens et des Electroniciens (France).

Chen Li received the B.Sc. degree in 1997 from the Precision Instrument and Mechatronics Department, Tsinghua University, Beijing, China, and the M.S. degree in mechanical engineering in 2000 from Clarkson University, Potsdam, NY, where he is currently working toward the Ph.D. degree.

His fields of interest include ultrasonics, signal analysis, and finite-element analysis.

Cetin Cetinkaya received the B.S. degree in aeronautical engineering from the Technical University of Istanbul, Istanbul, Turkey, in 1986, and the M.S. and Ph.D. degrees in aeronautical and astronautical engineering from the University of Illinois at Urbana-Champaign in 1991 and 1995, respectively.

He is an Associate Professor in the Department of Mechanical and Aeronautical Engineering at Clarkson University, Potsdam, NY. His areas of research interest include thermoelastic wave propagation nanoparticle adhesion and removal, acoustic/ultrasonic testing, laser-based nondestructive testing/evaluation, and vibration analysis.

Dr. Cetinkaya is a Member of the American Society of Mechanical Engineers.